The QED Engine System: Direct-Electric Fusion-Powered Rocket Propulsion Systems

By Robert W. Bussard, Energy/Matter Conversion Corporation, 680 Garcia Street, Santa Fe, NM 87505, (505) 988-8948, <emc2qed@comcast.net>

Abstract

Practical ground-to-orbit and inter-orbital space flights both require propulsion systems of large flight-path-averaged specific impulse (I_{sp}) and engine system thrust-to-mass ratio (F/m_e = $[F]$ for useful payload and structure tractions in single-stage vehicles[1]. Current rocket and air-breathing engine technologies lead to enormous vehicles and small payloads; a natural result of the limited specific energy available from chemical reactions. While nuclear energy far exceeds these specific energy limits[2], the inherent high-I_{sp} advantages of fission propulsion concepts for space and air-breathing flight[3] are negated for manned systems by the massive radiation shielding required by their high radiation output[4]. However, there are well-known radiation-free nuclear fusion reactions[5] between isotopes of selected light elements (such as H+^{11}B, D+^{3}He) that yield only energetic charged particles, whose energy can be converted directly into electricity by confining electric fields[6]. New confinement concepts using magnetic-electric-potentials[7] or inertial-collisional-compression (ICC)[8] have been found that offer the prospect of clean, compact fusion systems with very high output and low mass. Their radiation-free d.c. electrical output can power unique new electron-beam-driven thrust systems of extremely high performance. Parametric design studies show that such charged-particle electric-discharge engines ("QED" engines) might yield rocket propulsion systems with performance in the ranges of $2 < [F] < 6$ and $1500 < I_{sp} < 5500$ sec.

Background

The fusion-electric power source required to drive such rocket engines is based on the use of inertial-electrostatic confinement (IEC) of the desired fusion fuels[9]. Initial studies of IEC[10] used ions accelerated by grid potentials in spherically concentric devices (here called IXL systems) as small as 0.1 m in diameter. Large fusion reaction rate densities were obtained. The fuels were deuterium (D) and tritium (T), the two heavy isotopes of hydrogen; these produced copious quantities of energetic and hazardous neutrons according to the fusion reaction $D + T \rightarrow {}^4He + n$. This IXL type of system was inherently limited by drive power losses due to particle/grid collisions.

These limitations were overcome by:

(a) invention of a novel magnetic-electrostatic means for trapping of energetic electrons injected to produce a stable negative potential well for ion confinement called EXL systems,[7,11] and

(b) creation of a unique physics concept for stable electrostatic wave-group-trapping and subsequent inertial-collisional-compression (ICC) density enhancement of ions in a central core region[8].

These two new ideas formed the basis for revived IEC fusion research.

The Defense Research Advanced Projects Agency (DARPA) gave initial support[12] in 1984-1987, followed by an analytical and small-scale experimental effort during 1987/88 funded by the Strategic Defense Initiative Office through the Defense Nuclear Agency[13]. This showed the general feasibility of the new concepts and approach, through analysis of a comprehensive point model of the fusion device. A major program for further research and development was defined, and supported by the DARPA in 1989-1992. The most significant work under this program focussed on theoretical analyses, 1- and 2-D numerical computations, phenomenological modeling, and parametric design and systems studies of the EXL concept. Some experimental work was also undertaken on both IXL and EXL types of IEC system. Current research is supported by the US Navy, the Electric Power Research Institute, and the Department of Energy, Basic Energy Sciences Division through the Los Alamos National Laboratory (LANL). Both IEC concepts are shown in outline form in Figures 1a and 1b.

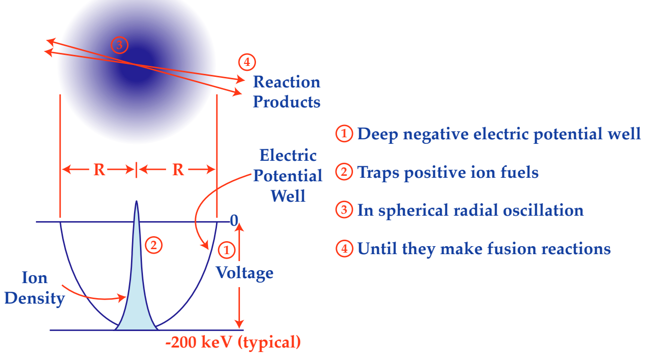

Figure 1a — Ion-injection IEC fusion system

Results of this recent work have shown that the new approaches are extremely promising, that there are no apparent "show-stoppers" or impossible physics or engineering obstacles to their success, and that they offer the prospect of very small-scale, clean (non-radiative) fusion-electric power by use of aneutronic fuels. The characteristics of both IXL and EXL systems are that they are all high voltage, with modest currents and small magnetic fields (none in the IXL system), and are inherently small in size. These features lead to low-cost and short time scale for the research required for their development. They are "low-technology" devices, but with "high-technology" physics.

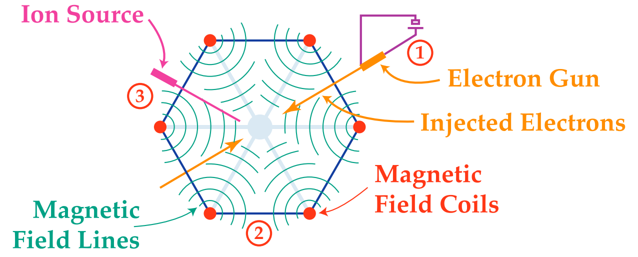

① Trapping well formed by energetic electron injection

② Cusps of polyhedral magnetic field

③ Ions fall into well and remain until reacted

Figure 1b — Electron-injection IEC system

Electrostatic Fusion Rocket Propulsion Systems

Fusion Fuels and Direct Conversion

To illustrate the prospects for fusion-electric rocket performance, consider only systems that operate on aneutronic fusion fuels. These include hydrogen (p) and boron-11 (${}^{11}B$), (p) and lithium-6 (${}^{6}Li$), deuterium (D) and helium-3 (${}^{3}He$), and ${}^{3}He$ ions alone. These reactions proceed as follows[14]:

$p + {}^{11}B$	—> $3\ {}^{4}He$	(8.7 MeV)
$p + {}^{6}Li$	—> ${}^{4}He + {}^{3}He$	(4.0 MeV)
${}^{3}He + {}^{6}Li$	—> $2\ {}^{4}He + p$	(16.9 MeV)
$D + {}^{3}He$	—> ${}^{4}He + p$	(18.3 MeV)
${}^{3}He + {}^{3}He$	—> ${}^{4}He + 2p$	(12.9 MeV)

The energy of these fusion product charged particles can be converted directly into electric power by causing them to expand against an electric field. Charged particles escaping radially from the center of the reaction sphere can drive current flow into spherical shell grid structures (to control decelerating voltage gradients) of opposing potentials surrounding the power-generating fusion core. The general feasibility of such direct conversion has been proven by earlier experimental research studies[15]. Its operating principles in the inertial-electrostatic-fusion power sources here are as shown in Figure 2.

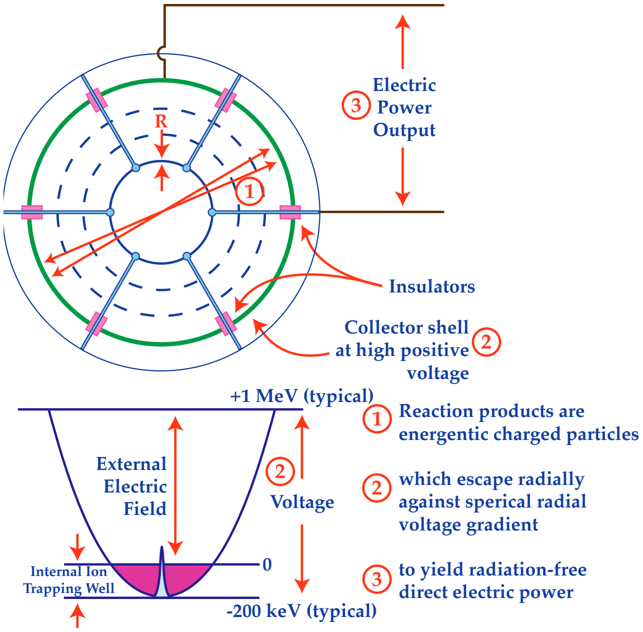

Figure 2 — Charged fusion product direct electric conversion

Output power from fusion product charged particles will appear as modest currents (kiloamps) at relatively high voltages (typically at 0.5-2 MeV), that can be used with little power conditioning to drive low-energy relativistic electron beams (reb) for propellant heating, as well as to power the fusion device, itself.

Electron-Beam Plasma / Propellant Heating

The energy carried by such beams can be deposited directly, essentially completely, into rotationally-confined high-pressure plasmas, on the axis of a cylindrical thrust chamber, producing very high gas/plasma temperatures. Thermal radiation from this core is absorbed by the radially inflowing fluid/gas/plasma, which then flows longitudinally along the system axis to a magnetically-insulated converging-diverging exhaust nozzle, to produce thrust at high I_{sp}. Chamber and nozzle wall insulation by use of axial magnetic fields in such reb-heated devices can reduce gas/wall heat transfer by up to two orders of magnitude from conventional convective processes[16]. The net effective specific impulse of hydrogen can then reach levels of I_{sp} = 2500 to 5500 sec (corresponding to temperatures of 20,000 to 80,000 K, depending on dissociation-recombination effects) without intractable wall cooling difficulties. Water, ammonia, methane, and other low molecular weight fluids can be driven to equally high I_{sp} levels, albeit at higher thrust chamber core gas temperatures. The operating chamber pressure must be optimized for energy deposition profiles to match propellant flow, with the achievement of optimum specific impulse from the exit gas, for the desired net thrust level of the system. Maximum I_{sp} will be obtained at pressures that promote some recombination of dissociated and ionized species in the nozzle flow. Such a combination of elements yields an reb-heated fusion-electric QED rocket propulsion system as shown in the block diagram of Figure 3.

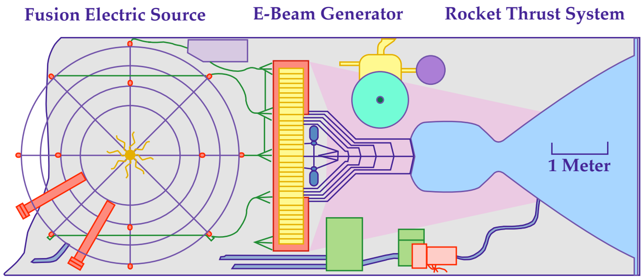

Figure 3 — Outline drawing of complete ARC/QED rocket engine system, showing basic components, structure, layout, and subsystems; fusion-electric source, electron beam generator; thrust system

The two keys to efficient heating are nearly-complete absorption of thermal radiation. in this process, and coupling of the reb into the central dense plasma. Beam/plasma coupling lengths must be small compared to the reb path through the propellant gas. Considerable study[17,18] has been given to the interaction of both high- and low-energy reb's with dense plasmas. Results[19] show that reb energy can be absorbed easily in QED thrust chambers of 0.5 m length, and the beam propagation can be coupled stably into the propellant. Only modest magnetic fields (typically 0.2-1.0 T; 2-10 kG) are needed to inhibit heat transfer to walls downstream of the heating region and to stabilize the propagating e-beam. Magnet coils for these guide and insulation fields can be located outside the chamber/nozzle structure and cooled cryogenIcally (by LH_2) before the propellant is sensibly heated by other regenerative heat loads.

Engine Configurations and Performance

Two approaches can be followed for QED engine configurations. First is an all regeneratively-cooled (ARC) system, in which that fraction of the fusion power not delivered to the e-beam and deposited into the propellant gas is taken up by the in-flowing propellant stream before entering the thrust chamber. Second is a system that utilizes a separate waste heat radiator (not shown in Figure 3) for controlled-space-radiation (CSR) cooling to handle some specified fraction of the regenerative cooling requirement. By this means the in-flowing propellant can reach higher final temperatures than in the ARC/QED engine system. The CSR mode is not considered further here. In the ARC mode the power and fluid flow scheme automatically limits the maximum propellant temperature (enthalpy) possible before expansion, and thus limits the I_{sp} attainable. If a fraction f_c of the total fusion power is deposited in structure constrained to a maximum temperature of 1800 C (2073 K), for example, this is given approximately by $I_{sp} = 1500/(f_c M)^{0.5}$ sec, where M is the average molecular weight of the dissociated propellant gases.

ARC/QED Engine Systems and Subsystems

The ARC system outlined in Figure 3 shows the engine system mass (me) in three major subsystems:

(1) Thrust system with mass m_{th};

(2) Fusion source with mass m_{fs}, and;

(3) Electric system with mass m_{el}

Each of these is made up of several sub-units. The thrust system includes the propellant turbopumps and associated bleed gas supply lines with mass m_{pe} and the thrust chamber subsystem of mass m_{tc} which includes the e-beam entrance diode assembly, a quasi-cylindrical heating chamber into which propellant is injected tangentially, for centrally-convergent centrifugal flow, and the guide and insulation magnet coils, embedded in or around the chamber and nozzle wall cooling channels. Analysis of design constraints and normalization to a single point design, gives a scaling algorithm for mass as:

$$m_{th} = m_{tc} + m_{pe} = \frac{400 P_0}{\sqrt{I_0}} + \left(\frac{P_0}{I_0}\right)^{1.67} + 40 \qquad (1)$$

where $P_o = P_f/2150$ is the ratio of total fusion power in MW, normalized to a point design value of 2150 MW, and I_o is the ratio of system specific impulse in seconds, normalized to a point design value of 3500 sec.

The fusion source is assumed to be an IXL type of IEC system. This device employs injection ion acceleration by biased grids, and achieves high core densities from the ICC wave-group-trapping effect. This system can be broken into four main sub-units; internal core structure m_{cs}, convertor grid structure m_{gr}, device shell (supports internal vacuum, and contains cooling channels) m_{sh}, and electric drive structure m_{ed}, for core drive. Analysis of each of these leads to an algorithm for the mass of this fusion-electric source as:

$$\begin{aligned} m_{fs} &= m_{cs} + m_{gr} + m_{sh} + m_{ed} \\ &= 250 P_0 + 550 (K_{iex}) \sqrt{P_0} + 600 (kg) \end{aligned} \tag{2}$$

The factor (K_{iex}) has been introduced here to account for the difference in mass between the IXL ion-injection and EXL electron-injection IEC systems. The IXL system has no magnets and $K_{iex} = 1$, while the magnetic fields required by the EXL system give a magnet coil and subsystem mass that scales as $K_{iex} = 10$. The performance analysis, following, is based on IXL system use.

Similarly, the main electric system breaks into two convenient sub-units, for electric voltage division and conversion m_{ce}, and for generation and transport of the e-beam m_{eb}. The electric system is then found to be:

$$m_{el} = m_{ce} + m_{eb} = 1800 P_0^{1.67} (kg) \tag{3}$$

With these, the total system mass becomes:

$$m_e = \sqrt{P_0}(550) + P_0 \left(250 + \frac{400}{\sqrt{I_0}} \right) + P_0^{1.67} \left[\frac{100}{I_0^{1.67}} + 1800 \right] + 640 (kg) \tag{4}$$

Overall System Performance

Table 1 — Example Point Design: ARC/QED Engine System

Subsystem/System Masses		Performance Parameters	
Thrust system	m_L = 540 kg	System	P_f = 2150 MW
	m_{pe} = 140 kg		P_L = 150MW
	m_{tc} = 400 kg		I_{spm} = 3500 sec
Fusion source	m_{fs} = 1400		F = 11,000 kg
	m_{cs} = 250 kg		m_e = 3,650 kg
	m_{gr} = 300 kg		kg[F] = (F/m_e) = 3.0
	(m_{mag} = 4950 kg)		a_{fes} = 1.74E-3 kg/kW
	m_{sh} = 600 kg		$1/a_{fes}$ = 575 kW/kg)
	m_{ed} = 250 kg	Fusion fuel = $p^{11}B$	
Electric system	m_{el} = 1800 kg	Fusion source dimensions	R_{core} = 1.75 m
	m_{ce} = 1200 kg		R_{grid} = 2.15 m
	m_{eb} = 600 kg		R_{shel} = 2.25 m
		Thrust chamber drive	E_{beam} = 500 keV
			I_{beam} = 4300 amps
		Propellant gas conditions	p_o = 1E7 dyne/cm^2 = 10 atm
Total System	m_e = 3740 kg		n_i = 3.5E17/cm^3 (+ 1.3x e-)

* magnet subsystem mass replaces grid mass shown if an EXL system is used

The point design parameters on which the scaling laws are based are summarized in Table 1, above. Scaling about these design values is valid over ranges of about $1000 < P_f < 6000$ Mw and $1500 < I_{sp} < 5500$ sec. The size of the QED reactor does not vary significantly over these ranges. There is a minimum size of internal core and electric conversion structure set by high voltage standoff requirements that can not practically be reduced. The upper power limit is determined by maximum feasible heat removal from core and grid structures for this size. The point design shown is optimistic but not impossible; as before, this is based on IXL system characteristics given success of an ICC mode of operation. If EXL operation is required, using a superconducting magnet version of the polyhedral magnetic-electric system, the mass of the cited point design system would be 8390 kg. For purposes of flight system performance estimation it is often useful to utilize a gross specific mass coefficient (a_{fes}) for the entire engine system, defined as:

$$m_e = a_{fes}(1000)P_f(kg) \qquad (5)$$

where a_{fes} is in units of kg/kW and P_f is in MW. This parameter provides a ready means of comparison with alternate electric propulsion systems. This parameter is NOT a universal constant, but depends on the values of

P_o and I_o. For the point design given, a_{fes} = 1.74E-3 kg/kW, for a specific power of 575 kW/kg. And finally:

$$F_0 = \frac{P_0}{I_0} \quad (6)$$

relates the system thrust, power, and specific impulse. Here $F_o = F/110{,}000$ is the ratio of thrust in Newtons (N) to a point design value of 110,000 N (11,000 kg). 'With this the engine system mass can be written in terms of I_{sp} and F (combining equations 4 and 6), giving the propulsion system thrust-to-mass ratio directly.

Parametric performance of the baseline IXL rocket engine system is shown in Figures 4 and 5, from Equations (1-6). Note that the engine system thrust-to-mass ratio [F] is in the range of 2-6 over the I_{sp} range of 1500-5500 sec. This performance is three or more orders of magnitude beyond that of any other high-I_{sp} engine system applicable to space propulsion.

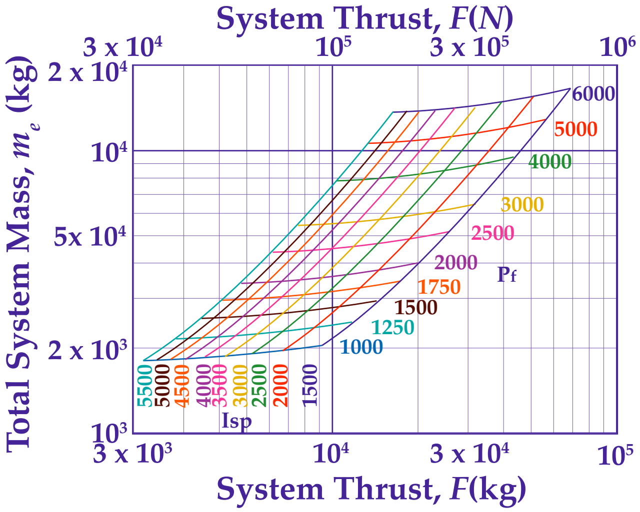

Figure 5 — ARC/QED engine system mass vs. thrust, for various values of power and specific impulse.

Aerospace Mission Performance

Single-Stage-To-Orbit (SSTO)

This engine system can be used for a horizontal-takeoff, single-stage-to-low-earth-orbit (LEO) mission in a vehicle of the type shown in Figure 6. This uses conventional turbojet engines for flight propulsion to M = 2.5, and then switches over to QED rocket propulsion.

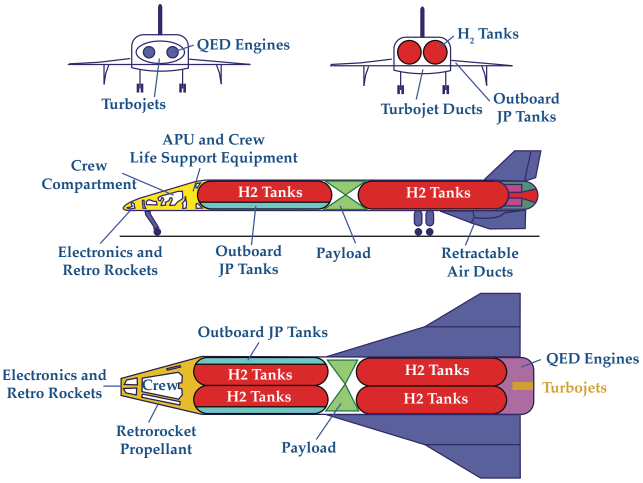

Figure 6 — Schematic outline inboard profile of single-stage-to-orbit (SSTO) QED engine driven vehicle, for LH_2 propellant, with assumed gross takeoff weight (GTOW) of 125,000 kg. Use of NH_3 propellant would result in smaller vehicle size.

Vehicle flight performance was estimated from the exponential mass-ratio equation, using a net effective specific impulse (I_s) of the engine system ***in the vehicle drag environment*** determined over its flight path to orbit. A flight trajectory was assumed that maintained a slowly monotonically-decreasing dynamic pressure after engine switch-over to the QED rocket mode, up to about Mach 10. At this point the vehicle attitude was increased for more rapid altitude gain with rapidly decreasing dynamic pressure and drag (D). Taking the turbojet engine thrust/mass ratio to be $(F/m_e)_{tj} = 8$, and analyzing vehicle drag at hypersonic speeds from simplified flat plate models allowed estimation of the variation of vehicle system (F/m_e) and (D/F) ratios along the flight path. The local I_s was then determined from the engine I_{sp} as $I_s = I_{sp}[1-(D/F)]$. This is shown in Figure 7, for the assumed flight trajectory. For comparison, subsonic and supersonic-burning ramjet net I_s curves are also shown. Note that the flight-speed-averaged value is $2200 < I_s < 2400$ sec; comparable to performance of the subsonic turbojet engines.

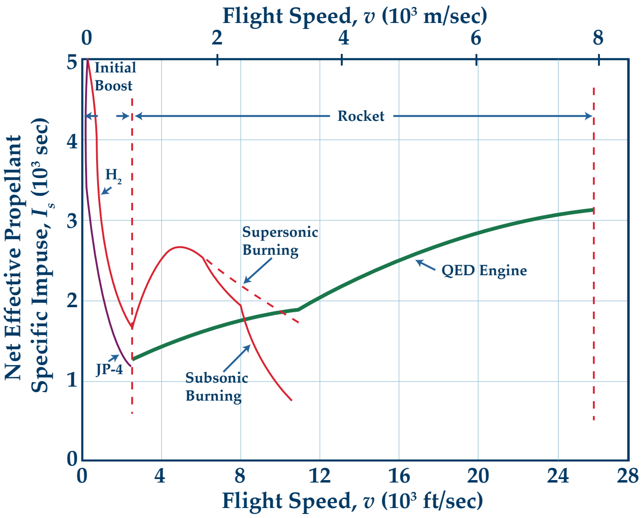

Figure 7 — Vehicle system net effective specific impulse, including effects of system drag and engine thrust loss over flight speed range

Using this variation of I_s, the mass fraction remaining and vehicle flight speed were computed as a function of flight time, as shown in Figure 8. Burnout occurs at about 20 minutes (1200 sec), followed by a 45 minute (2730 sec) coast to apogee at 555 km (300 nautical miles), and a thrust increment to add about 107 m/sec (350 ft/sec) for orbit circularization. The orbital mass fraction remaining in low earth orbit is about 0.62 of gross take-off mass (GTOM) (m_0); ample margin for large payload capacity with sturdy structure factors. Other, independent studies of this vehicle show a lesser mass of about 0.52 GTOM. However, even these allow dramatic reductions in payload delivery costs to LEO with ARC/QED engine system use.

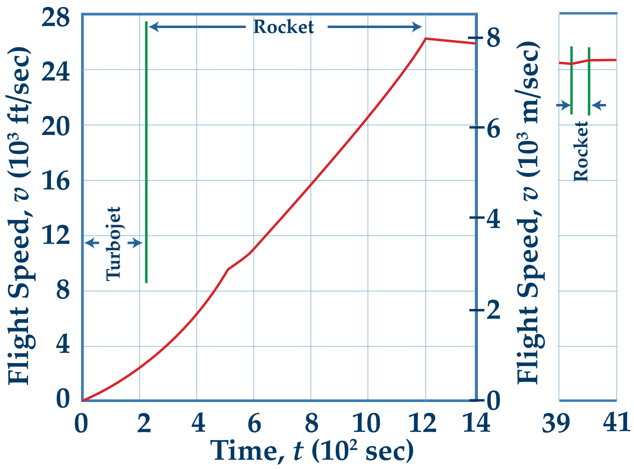

Figure 8a — Vehicle flight performance using QED engines, showing flight speed as functions of flight time

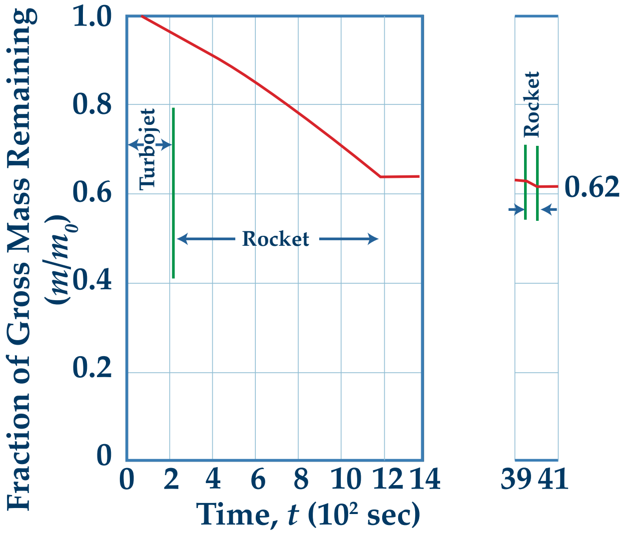

Figure 8b — Vehicle flight performance using QED engines, showing gross mass remaining as functions of flight time

Single-Stage Earth-Mars Flight

Interplanetary flight offers still more attractive possibilities, largely because the transit times for such flights can be reduced drastically from those expected for conventional chemical or nuclear-thermal missions, while still allowing use of single-stage systems. This is a direct result of the very much larger propellant specific impulse available from the QED engine system than from other high-thrust engine options. Vehicle characteristic incremental velocity capability is simply increased by the ratio of net effective I_s values between systems.

Analyses were made of the use of QED/ARC engines for flight of single-stage vehicles from the Earth's solar orbit to the orbit of Mars, with circularization at the Martian orbit (but not including Martian gravity capture). Results of this showed that a minimum vehicle with an initial mass of 500 tonnes could fly to Mars' orbit in 39.9 days with 103 tonnes (20.6%) of useful payload, or in 33.2 days (using 12.5 times the thrust) with 72 tonnes (14.4%) payload. Both vehicles fly as "high-thrust" spacecraft, under force accelerations one to two orders of magnitude larger than the local acceleration of the sun's gravity field throughout the flight. Studies of other interplanetary missions show similarly astonishing performance.

Conclusions

New concepts for electrostatic confinement and control of fusion reactions between non-radiative fusionable fuels offer propulsion systems of superior aerospace flight performance capabilities for trans-atmospheric and interplanetary and Earth/Moon space flight. If feasible, these QED engines could give performance two to four orders of magnitude better than that attainable from any other “conventional” aerospace chemical, nuclear-thermal, or electric propulsion systems. Fusion-electric QED engines typically have $2 < [F] < 6$ and $1500 < I_{sp} < 5500$ sec, and thus offer both “high-I_{sp}” and “high-thrust” capabilities. With these engines, space transport costs could be reduced to levels comparable to those of current high-speed aircraft and space flight would become economically attractive, widely available and practical, at last.

Acknowledgments

The work presented here was done at Energy/Matter Conversion Corporation (EMC2) under internal funding. Informal support also was given by Dr. R.H.W. Waesche of the Atlantic Research Corporation, who prepared the drawing of the QED/ARC engine, and by Dr. Dana Andrews of the Boeing Space and Defense Group, who carried out computer-based flight studies of the QED/ARC-engine-powered SSTO vehicle. The author wishes to express his appreciation to these colleagues for their interest and work.

Revision History

Published on January 20, 1993 in the American Institute of Physics (AIP) Conference Proceedings of the Tenth Symposium on Space Nuclear Power and Propulsion, Volume 271, pp. 1601-1612.

Reformatted and color illustrations added August 2007 by Mark Duncan. Minor updates to equations and illustrations in December 2008, and references in April 2009.

References

[1] Maxwell Hunter, “Solar System Spaceships,” in *Thrust Into Space*, Holt, Rhinehart and Winston, New York, Chapter 5.

[2] Robert W. Bussard and Richard D. DeLauer, *Nuclear Rocket Propulsion*, McGraw-Hill Book Co., New York.

[3] Robert W. Bussard and Richard D. DeLauer, *Fundamentals of Nuclear Flight*, McGraw-Hill Book Co., New York.

[4] Robert W. Bussard, “ASPEN-II: Two-staging and Radiation Shielding Effects on ASPEN Vehicle Performance,” LA-2680, June 25, 1962, declassified with deletions September 6, 1967; later summarized in “ASPEN: Nuclear Propulsion for Earth-to-Orbit Aerospace Plane Vehicles,” Robert W. Bussard, Proceedings International Conference on Space Technology, Rome, June 1971.

[5] Robert A. Gross, “Fusion Energy,” John Wiley & Sons, Inc., New York, Appendix C. ISBN 0-471-88470-7

[6] Ralph W. Moir and William L. Barr, “Test Results on Plasma Direct Convertors,” Nuclear Technology and Fusion, Volume 3, 1983, p.98.

[7] Robert W. Bussard, “Method and Apparatus For Controlling Charged Particles,” U.S. Patent No. 4,826,626, 2 May 1989, to Energy/Matter Conversion Corp. (EMC2), Manassas, VA.

[8] Robert W. Bussard, “Method and Apparatus for Creating and Controlling Nuclear Fusion Reactions.” U.S. Patent 5,160,695, assigned to QED, Inc., Greenbelt, MD, November 3, 1992.

[9] William C. Elmore, James L. Tuck, and Kenneth M. Watson, “On the Inertial-Electrostatic Confinement of a Plasma,” Physics Fluids. Volume 2, Number 3, May-June 1959, p. 239.

[10] Robert L. Hirsch, “Inertial-Electrostatic Confinement of Ionized Fusion Gases,” Journal Applied Physics, Volume 38, Number 11, October 1967, p. 4522.

[11] Robert W. Bussard, “Some Physics Considerations of Magnetic Inertial-Electrostatic Confinement - A New Concept for Spherical Converging-Flow Fusion,” Fusion Technology, Volume 19, March 1991, p. 273.

[12] Robert W. Bussard “Final Report; DARPA/BMI Study of Advanced Energy Sources and Systems: New Alternatives for Tactical Applications(U), Volume I, A New Method for Control of Charged Particle Interactions(U),” Final Report PSR- 1709, December 31, 1986, Contract No. DAAH01-84-Q005, Battelle Columbus Division, for DARPA, U.S. Department of Defense, Pacific-Sierra Research Corp., Arlington, VA, revised March 1987.

[13] Robert W. Bussard, G.P. Jellison, and G.E. McClelland, “Preliminary Research Studies of a New Method for Control of Charged Particle Interactions,” Final Report PSR-1899, 30 November 1988, Contract No. DNA001-87-C-0052, Defense Nuclear Agency, revised March 1989.

[14] David L. Book, *NRL Plasma Formulary* (1983 Revision), Naval Research Laboratory, Washington D.C.

[15] Ralph W. Moir and William L. Barr “’Venetian Blind’ Direct Energy Convertor for Fusion Reactors,” Nuclear Fusion, Volume 13, 1973, p.35.

[16] Richard A. Gerwin; George J. Marklin; Anthony G. Sgro; Alan H. Glasser; “Characterization of Plasma Flow Through Magnetic Nozzles”, Report # AL-TR-89-092, Air Force Astronautics Lab, EAFB, CA, February 1990.

[17] Lester E. Thode and Ravi N. Sudan, “Plasma heating by relativistic electron beams. I. Two-stream instability, and; II. Return current interaction,” Physics Fluids, Volume 18, Number 11, November 1975, p. 1552, 1564; doi: 10.1063/1.861053

[18] Ronald C. Davidson, *Theory of Nonneutral Plasmas*, W.A. Benjamin, Inc., Reading, MA, 1974, Section 2.11, p. 78 ff.

[19] Lester E. Thode “Effect of Electron-Ion Collisions on the Nonlinear State of the Relativistic Two-stream Instability,” Physics Fluids, Volume 20, Number 12, 1977, p. 2121; doi: 10.1063/1.861842